

Rogue waves, rational solutions, the patterns of their zeros and integral relations

This article has been downloaded from IOPscience. Please scroll down to see the full text article.

2010 J. Phys. A: Math. Theor. 43 122002

(<http://iopscience.iop.org/1751-8121/43/12/122002>)

View [the table of contents for this issue](#), or go to the [journal homepage](#) for more

Download details:

IP Address: 171.66.16.157

The article was downloaded on 03/06/2010 at 08:41

Please note that [terms and conditions apply](#).

FAST TRACK COMMUNICATION

Rogue waves, rational solutions, the patterns of their zeros and integral relations

Adrian Ankiewicz¹, Peter A Clarkson² and Nail Akhmediev¹¹ Optical Sciences Group, Research School of Physics and Engineering, Institute of Advanced Studies, The Australian National University, Canberra ACT 0200, Australia² School of Mathematics, Statistics and Actuarial Science, University of Kent, Canterbury, CT2 7NF, UKE-mail: ana124@rsphysse.anu.edu.au, P.A.Clarkson@kent.ac.uk and mna124@rsphysse.anu.edu.au

Received 8 December 2009, in final form 10 February 2010

Published 3 March 2010

Online at stacks.iop.org/JPhysA/43/122002**Abstract**

The focusing nonlinear Schrödinger equation, which describes generic nonlinear phenomena, including waves in the deep ocean and light pulses in optical fibres, supports a whole hierarchy of recently discovered rational solutions. We present recurrence relations for the hierarchy, the pattern of zeros for each solution and a set of integral relations which characterizes them.

PACS numbers: 42.65.-k, 47.20.Ky, 47.25.Qv

(Some figures in this article are in colour only in the electronic version)

1. Introduction

'Rogue waves' are giant single waves appearing in the ocean [16]. The average height of rogue waves is at least twice the height of the surrounding waves. Thus, they can be quite unexpected and mysterious. In recent years, the idea of rogue waves has been extended far beyond oceanic expanses. The concept has been applied to pulses emerging from optical fibres [12, 20], waves in Bose–Einstein condensates [6], in superfluids [13], in optical cavities [15], in the atmosphere [21] and even in finance [22]. One possible mathematical model for rogue waves uses rational solutions of the nonlinear Schrödinger equation (NLSE) [4]. Indeed, the focusing NLSE [1] is applicable to deep water waves [23] as well as to a variety of other nonlinear phenomena. In dimensionless form it can be written as

$$i \frac{\partial \psi}{\partial t} + \frac{\partial^2 \psi}{\partial x^2} + \frac{1}{2} |\psi|^2 \psi = 0, \quad (1)$$

where ψ is the wave envelope, t is the temporal variable and x is the spatial variable in the frame moving with the wave. Note that the coefficients in equation (1) are different from those

used in [1, 4] in the meaning and scaling of the variables. Namely, we have made a re-scaling and swap of the variables: $x \rightarrow t/2$ and $t \rightarrow x/2$. This transformation allows us to present the solutions in somewhat simpler forms and to relate them to other solutions.

The focusing NLSE (1) has a variety of solutions and among them there is a hierarchy of rational solutions that are localized in both the x and t variables. The method for generating them has been presented recently in [2]. Each solution of the hierarchy represents a unique event in space and time, as it increases its amplitude quickly along each variable, reaches its maximum value and finally decays, just as quickly as it appeared. Thus, these waves were nicknamed ‘waves that appear from nowhere and disappear without a trace’ [4]. The concept ‘collisions of Akhmediev breathers’ is an alternative description of rogue waves [3, 5]. As rational solutions are limiting cases of Akhmediev breathers, these two models produce generally similar results.

Qualitatively different types of rational solutions attributed to the *defocusing* NLSE,

$$i \frac{\partial \psi}{\partial t} + \frac{\partial^2 \psi}{\partial x^2} - \frac{1}{2} |\psi|^2 \psi = 0, \quad (2)$$

have been studied in [9, 14, 17]; a major point is that such rational solutions are singular. Similar types of rational solutions for the Boussinesq equation and the classical Boussinesq system have also been studied in [10] and [11], respectively. For the defocusing NLSE (2), there are rational solutions of the form

$$\psi(x, t) = g(x, t)/f(x, t), \quad (3)$$

and rational oscillatory solutions of the form

$$\psi(x, t) = \frac{g(x, t)}{f(x, t)} \exp\left(-\frac{ix^2}{6t}\right), \quad (4)$$

where $g(x, t)$ and $f(x, t)$ are polynomials in the variables x and t . Their expressions have been derived and the pattern of poles and zeros has been analysed in [9]. Rational solutions of the form (3) are expressed in terms of the ‘generalized Hermite polynomials’ [18] and rational solutions of the form (4) are expressed in terms of the ‘generalized Okamoto polynomials’ [18]. These generalized Hermite and generalized Okamoto polynomials are forms of Schur polynomials which arise in the description of rational solutions of the fourth Painlevé equation and their roots have an intriguing, highly symmetric and regular structure in the complex plane [7–9].

Our aim in this work is to apply the technique of constructing the patterns of zeros of rational solutions developed for the defocusing NLSE to the case of the focusing NLSE. These patterns, besides being a work of art by themselves, have the advantage that they allow us to derive certain integral relations. The determination of the sequence of rational solutions of the NLSE (1), which take the form

$$\psi(x, t) = \frac{g(x, t)}{f(x, t)} \exp\left(\frac{1}{2}it\right), \quad (5)$$

involves modifying the Darboux procedure [1], so that each solution is found from the previous one, using intermediate functions which are found by directly solving a linear set of equations whose compatibility condition is the NLSE [2]. The rational solutions of the focusing NLSE (1) of the form (5), given in [2], differ dramatically from the solutions of those of the defocusing NLSE (2) in that the denominators $f(x, t)$ are real and positive for all real x and t , so the resulting wave forms are finite everywhere. However, the polynomials $f(x, 0)$ have zeros for complex values of x and finding the patterns of their appearance is one of our goals.

2. Analysis

The most convenient way to write each rational solution is

$$\psi_j(x, t) = \left\{ (-1)^j + \frac{G_j(x, t) + itH_j(x, t)}{F_j(x, t)} \right\} \exp\left(\frac{1}{2}it\right), \tag{6}$$

where $G_j(x, t)$, $H_j(x, t)$ and $F_j(x, t)$ are polynomials in x and t , and $F_j(x, t)$ has no real zeros. In this communication, we are concerned explicitly with the cases when $j \leq 5$. In particular, for $j = 1$ we have

$$G_1(x, t) = 4, \quad H_1(x, t) = 4, \quad F_1(x, t) = 1 + x^2 + t^2,$$

[4, 19]³. Any solution of the NLSE can be multiplied by an arbitrary phase factor. We take $\psi_j(0, 0) > 0$, and this means that we require $G_j(0, 0) > 0$, since $F_j(x, t) > 0$ for all x and t . These waves can be generated from random initial conditions on a unit background, i.e. flat sea level [3]. For $j = 2$ we have

$$\begin{aligned} G_2(x, t) &= -12\{x^4 + 6(t^2 + 1)x^2 + 5t^4 + 18t^2 - 3\}, \\ H_2(x, t) &= -12\{x^4 + 2(t^2 - 3)x^2 + (t^2 + 5)(t^2 - 3)\}, \\ F_2(x, t) &= x^6 + 3(t^2 + 1)x^4 + 3(t^2 - 3)^2x^2 + t^6 + 27t^4 + 99t^2 + 9. \end{aligned}$$

Higher order solutions are progressively more complicated. Finding simple ways to derive them is one of the challenges that we face.

It turns out that we can generate the functions $G_j(x, 0)$ and $F_j(x, 0)$, i.e. the forms on the x -axis, by using the recurrence relations (7) and (8) below. First, we generate $F_j(x, 0)$ using the differential–difference equation

$$F_{j+1}(x, 0)F_{j-1}(x, 0) = \{x^2 + (2j + 1)^2\}F_j^2(x, 0) + 4x^2\{F_j(x, 0)F_{j,xx}(x, 0) - F_{j,x}^2(x, 0)\}, \tag{7}$$

for $j \geq 1$, with $F_0(x, 0) = 1$ and $F_1(x, 0) = 1 + x^2$ and

$$F_{j,x} \equiv \frac{\partial F_j}{\partial x}, \quad F_{j,xx} \equiv \frac{\partial^2 F_j}{\partial x^2}.$$

We remark that differential–difference equations similar to (7) arise in the description of polynomials associated with rational solutions of the Painlevé equations; see [8] and the references therein.

Given $F_j(x, 0)$, we obtain $G_j(x, 0)$ using

$$G_j(x, 0) = (-1)^{j+1} \left\{ F_j(x, 0) - \left[4F_j(x, 0)F_{j,xx}(x, 0) - 4F_{j,x}^2(x, 0) + F_j^2(x, 0) \right]^{1/2} \right\}, \tag{8}$$

which can be derived from the bilinear representation of the NLSE (1), see [17]. Since $\deg(G) = \deg(F) - 2$, where $\deg(G)$ and $\deg(F)$ respectively are the degrees of the polynomials $G_j(x, 0)$ and $F_j(x, 0)$ (see table 1), then the sign of the square root in equation (8) is critical.

Using (7) and (8) we can determine $\psi_j(x, 0)$ for all j . For $j = 1$, the numerator and denominator polynomials respectively are

$$G_1(x, 0) = 4, \quad F_1(x, 0) = 1 + x^2.$$

For $j = 2$ we have

$$G_2(x, 0) = -12(x^4 + 6x^2 - 3), \quad F_2(x, 0) = x^6 + 3x^4 + 27x^2 + 9,$$

³ See <http://demonstrations.wolfram.com/RogueOceanWaves/> for an interactive demonstration.

Table 1. Characteristics of rational solutions. Here, $\deg(G)$, $\deg(H)$ and $\deg(F)$ are the degrees of the polynomials $G_j(x, 0)$, $H_j(x, 0)$ and $F_j(x, 0)$. Finally ‘ $\psi_j(x, 0)$ real zeros’ is the number of real zeros on the line $t = 0$.

j	$\deg(G) = \deg(H)$	$\deg(F)$	$\psi_j(x, 0)$ real zeros
1	0	2	2
2	4	6	4
3	10	12	6
4	18	20	8
5	28	30	10
j	$(j - 1)(j + 2)$	$j(j + 1)$	$2j$

for $j = 3$

$$G_3(x, 0) = 24(x^{10} + 15x^8 + 210x^6 - 450x^4 - 675x^2 + 675),$$

$$F_3(x, 0) = x^{12} + 6x^{10} + 135x^8 + 2340x^6 + 3375x^4 + 12150x^2 + 2025,$$

for $j = 4$

$$G_4(x, 0) = -40(x^{18} + 27x^{16} + 900x^{14} + 18900x^{12} - 10730x^{10} - 481950x^8 - 1190700x^6 + 17860500x^4 + 22325625x^2 - 4465125),$$

$$F_4(x, 0) = x^{20} + 10x^{18} + 405x^{16} + 16200x^{14} + 425250x^{12} + 1644300x^{10} + 17435250x^8 + 130977000x^6 + 111628125x^4 + 223256250x^2 + 22325625,$$

and finally, for $j = 5$

$$G_5(x, 0) = 60(x^{28} + 42x^{26} + 2415x^{24} + 119700x^{22} + 3221505x^{20} - 40153050x^{18} - 370010025x^{16} - 2893401000x^{14} + 30787036875x^{12} + 1299806817750x^{10} + 5540260123125x^8 + 17840228332500x^6 - 21709549378125x^4 - 13291560843750x^2 + 3987468253125),$$

$$F_5(x, 0) = x^{30} + 15x^{28} + 945x^{26} + 64575x^{24} + 3709125x^{22} + 133656075x^{20} + 1115785125x^{18} + 24214372875x^{16} + 463546951875x^{14} + 5581517878125x^{12} + 14657286301875x^{10} + 93610564228125x^8 + 412481438184375x^6 + 232602314765625x^4 + 299060118984375x^2 + 19937341265625.$$

The central maximum for each of the above solutions is given by

$$\psi_j(0, 0) = (-1)^j + \frac{G_j(0, 0)}{F_j(0, 0)} = 2j + 1,$$

and the number of zeros of $\psi_j(0, 0)$ on the line $t = 0$ is $2j$. The background magnitude level is always 1. The latter can be considered as a reference point for the amplitudes. Any deviation from the background level is an excitation. Thus, the ‘energy’ of an excitation also has to be calculated starting from the background level. This has to be distinguished from the usual definition of energy which is infinite for any solution with a nonzero background.

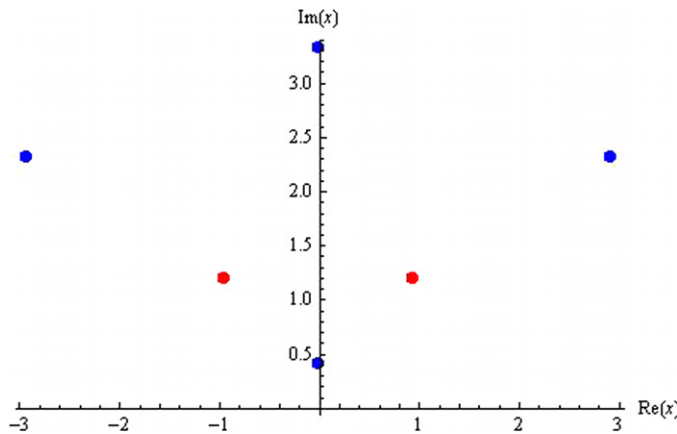


Figure 1. The six upper half plane zeros of $F_3(x, 0)$, i.e. poles of G_3/F_3 , from the third-order rational solution. Poles with residue $+2i$ are marked with red dots, while those with residue $-2i$ are marked with blue dots.

3. First relation

Using the Hirota representation of the NLSE, it can be shown that

$$\int_{-\infty}^{\infty} \{ |\psi_j(x, t)|^2 - 1 \} dx = 0, \tag{9}$$

for all x , so that ‘energy’ of the excitation is conserved [4], thus verifying a well-known conserved quantity of the NLSE. The above equation is also a manifestation of the fact that amounts of excitation $|\psi_j(x, t)|^2$ above and below the background level are equal.

We now try to understand the following curious relation. Using equation (6), following [2] we define

$$M_j = \int_{-\infty}^{\infty} \{ \psi_j(x, 0) - (-1)^j \} dx = \int_{-\infty}^{\infty} R_j(x) dx, \tag{10}$$

where $R_j(x) = G_j(x, 0)/F_j(x, 0)$. Comparison with equation (9) shows that M_j is an integral of the excitation above the background level. Further, in contrast to (9), the integral with infinite limits in this case is non-zero. We use complex analysis to evaluate the residues of zeros of the polynomials $F_j(x, 0)$ in the upper half complex x plane. The residue of $R_j(x)$ at one of its poles, say x_k , is

$$\text{Res}(R_j)_{x=x_k} = G_j(x_k, 0)/F_{j,x}(x_k, 0).$$

For $j = 1$, the zeros of $F_1(x, 0)$ are at $x = \pm i$, so the residue at $x = \pm i$ is $\mp 2i$. From equation (8) we have

$$G_j^2(x, 0) - 2(-1)^{j+1} F_j(x, 0) G_j(x, 0) = 4 \{ F_j(x, 0) F_{j,xx}(x, 0) - F_{j,x}^2(x, 0) \}, \tag{11}$$

which on setting $x = x_k$ implies that

$$G_j^2(x_k, 0) = -4 F_{j,x}^2(x_k, 0),$$

and so

$$\text{Res}(R_j)_{x=x_k} = \pm 2i. \tag{12}$$

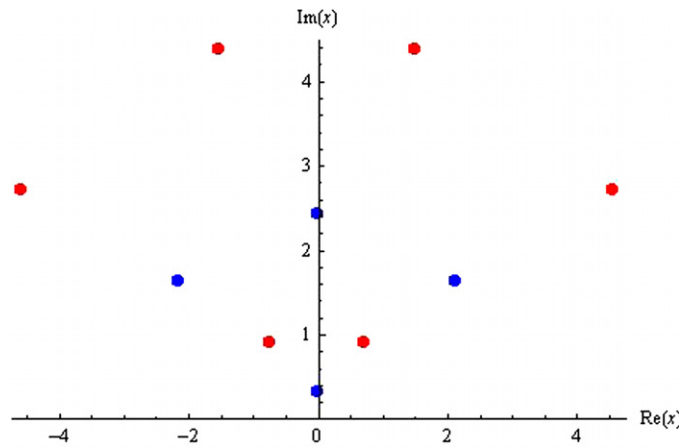


Figure 2. The ten upper half plane zeros of $F_4(x, 0)$ from the fourth-order rational solution. Poles of G_4/F_4 with residue $+2i$ are marked with red dots, while those with residue $-2i$ are marked with blue dots. This looks like a scaled version of figure 1 with an additional upper red arc.

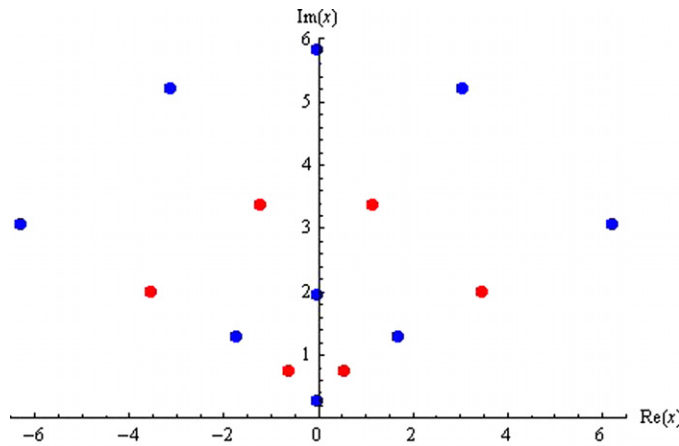


Figure 3. The 15 upper half plane zeros of $F_5(x, 0)$ from the fifth-order rational solution. Poles of G_5/F_5 with residue $+2i$ are marked with red dots, while those with residue $-2i$ are marked with blue dots. This resembles a scaled version of figure 2 with an additional upper blue arc.

Thus, for all values of j , every residue of $R_j(x)$ is $\pm 2i$. This is a rather amazing feature and we can then find M_j easily by summing these residues. The zeros form arcs, as can be seen in figures 2 and 3. The inner arc, i.e. the lowest blue dot in each diagram, has one zero (residue $-2i$), the second arc has two zeros (each residue $+2i$), and so on, and the final j th arc has j zeros. There are $\frac{1}{2}j(j+1)$ zeros in both the upper half plane and the lower half plane. The total number of zeros, namely $j(j+1)$, of course, matches the order of the polynomial $F_j(x, 0)$. The integral can be found from the total residue. Thus,

$$M_j = 2\pi \sum_{k=1}^j (-1)^{k+1} k = \pi [1 - (-1)^j (1 + 2j)]$$

$$= \begin{cases} 2(j+1)\pi, & \text{for } j \text{ odd,} \\ -2j\pi, & \text{for } j \text{ even,} \end{cases}$$

which are easily verified by numerical integration.

4. Second relation

We now define the integral of the square of excitation above the background level

$$\begin{aligned}
 S_j &= \int_{-\infty}^{\infty} \{\psi_j(x, 0) - (-1)^j\}^2 dx \\
 &= \int_{-\infty}^{\infty} \left\{ \frac{G_j(x, 0)}{F_j(x, 0)} \right\}^2 dx = \int_{-\infty}^{\infty} R_j^2(x) dx.
 \end{aligned}
 \tag{13}$$

The poles are located in the same places on the complex x plane, but now each is of order 2.

Thus, we now use the residue definition for a pole at $x = x_k$

$$\text{Res}(R_j^2) = \lim_{x \rightarrow x_k} \frac{d}{dx} \{(x - x_k)^2 R_j^2(x)\}, \quad k = 1, 2, \dots, \frac{1}{2}j(j+1)$$

i.e. for each of the upper half x -plane poles. To determine the residue at $x = x_k$, a root of $F_j(x, 0)$, we let $F_j(x, 0) = (x - x_k)f_j(x)$ and $G_j(x, 0) = g_j(x)$. Then,

$$\begin{aligned}
 \lim_{x \rightarrow x_k} \frac{d}{dx} \{(x - x_k)^2 R_j^2(x)\} &= \lim_{x \rightarrow x_k} \frac{d}{dx} \left\{ \frac{g_j^2(x)}{f_j^2(x)} \right\} \\
 &= \frac{2g_j(x_k)}{f_j^2(x_k)} \frac{dg_j}{dx}(x_k) - \frac{2g_j^2(x_k)}{f_j^3(x_k)} \frac{df_j}{dx}(x_k).
 \end{aligned}$$

From equation (11) we have $g_j^2(x_k) = -4f_j^2(x_k)$ and

$$g_j(x_k) \frac{dg_j}{dx}(x_k) = (-1)^{j+1} f_j(x_k) g_j(x_k) - 4f_j(x_k) \frac{df_j}{dx}(x_k),$$

and therefore

$$\text{Res}(R_j^2) = \frac{2(-1)^{j+1} g_j(x_k)}{f_j(x_k)} = \frac{2(-1)^{j+1} G_j(x_k, 0)}{F_{j,x}(x_k, 0)} = \pm 4i.$$

Here, the pole on the upper half plane with the lowest imaginary part has residue $4i(-1)^j$, while the two poles on the next arc each have residue $4i(-1)^{j+1}$ and the three poles on the next arc each have residue $4i(-1)^j$.

The above could be used in generalizations to higher powers of R_j . However, we can obtain the S_j result easily by expanding the square in the integrand of S_j and using equation (9). This gives

$$\int_{-\infty}^{\infty} R_j^2(x) dx = 2(-1)^{j+1} \int_{-\infty}^{\infty} R_j(x) dx,
 \tag{14}$$

and so

$$S_j = 2(-1)^{j+1} M_j.
 \tag{15}$$

Either way, we find that

$$\begin{aligned}
 S_j &= 8\pi(-1)^j \sum_{k=1}^j (-1)^k k = 2\pi \{2j + 1 - (-1)^j\} \\
 &= \begin{cases} 4(j+1)\pi, & \text{for } j \text{ odd,} \\ 4j\pi, & \text{for } j \text{ even,} \end{cases}
 \end{aligned}$$

which are also easily verified by numerical integration. Thus, S_j/π is always a positive integer and is equal to $2R_j(0)$, as indicated in the second column of table 2.

Table 2. Characteristics of rational solutions. Here, $\psi_j(0, 0)$ is the overall maximum amplitude of the rogue wave. We note that M_j , given by equation (10), and S_j , given by equation (13), are always multiples of 2π .

j	$R_j(0) = \frac{G_j(0,0)}{F_j(0,0)} = \frac{S_j}{2\pi}$	$\psi_j(0, 0)$	$\frac{M_j}{\pi}$
1	4	3	4
2	4	5	-4
3	8	7	8
4	8	9	-8
5	12	11	12
j	$2j + 1 - (-1)^j$	$2j + 1$	$1 - (-1)^j (1 + 2j)$

If we define

$$I_k = \int_{-\infty}^{\infty} \frac{dx}{(1+x^2)^k},$$

then, using integration by parts, it can be shown that for $k \geq 1$, I_k satisfies the recurrence relation

$$I_{k+1} = \frac{2(2k-1)}{k} I_k, \quad k \geq 1,$$

with $I_1 = \pi$. Thus, since $R_1(x) = 4/(1+x^2)$, then

$$\int_{-\infty}^{\infty} R_1^k(x) dx = 2^{k+1} \pi \frac{(2k-3)!!}{(k-1)!}, \quad k \geq 1,$$

where $(2k-3)!!$ is the double factorial given by

$$(2k-3)!! = \prod_{j=1}^{k-1} (2j-1) \equiv 2^{k-1} \pi^{-1/2} \Gamma\left(k - \frac{1}{2}\right)$$

with $\Gamma(k)$ the Gamma function. However, there appear to be no simple results for $j > 1$. The fact that these integrals, involving ratios of polynomials, turn out to be integer multiples of π emphasizes the proposition that these solutions are new fundamental objects. It is reminiscent of results involving π which appear in integrals of orthogonal polynomials. For example, we note that

$$\int_{-\infty}^{\infty} H_n^2(x) \exp(-x^2) dx = 2^n n! \sqrt{\pi},$$

where $H_n(x)$ is the Hermite polynomial of order n .

Rogue waves can have applications in various areas of science. Each has a distinct value of M_j , so this integral can be used to classify members of the hierarchy.

5. Conclusions

In conclusion, we have found recurrence relations for the hierarchy of rational solutions of the focusing nonlinear Schrödinger equation that describe rogue waves in the deep ocean. These relations are useful in obtaining higher order solutions of the hierarchy and in analysing the patterns of their poles. Knowledge of the poles and their properties can be used to derive integral relations for the excitation of these solutions above the background level. Here, we have derived two amplitude relations and expressed them in terms of the order of the solution.

Acknowledgments

The authors acknowledge the support of the Australian Research Council (Discovery Project DP0663216). They also thank the referee for some detailed comments which have improved the manuscript.

References

- [1] Akhmediev N and Ankiewicz A 1997 *Solitons, Nonlinear Pulses and Beams* (London: Chapman and Hall)
- [2] Akhmediev N, Ankiewicz A and Soto-Crespo J M 2009 *Phys. Rev. E* **80** 026601
- [3] Akhmediev N, Ankiewicz A and Soto-Crespo J M 2009 *Phys. Lett. A* **373** 2137–45
- [4] Akhmediev N, Ankiewicz A and Taki M 2009 *Phys. Lett. A* **373** 675–8
- [5] Akhmediev N, Soto-Crespo J M and Ankiewicz A 2009 *Phys. Rev. A* **80** 043818
- [6] Bludov Y V, Konotop V V and Akhmediev N 2009 *Phys. Rev. A* **80** 033610
- [7] Clarkson P A 2003 *J. Math. Phys.* **44** 5350–74
- [8] Clarkson P A 2006 *Comput. Methods Funct. Theory* **6** 329–401
- [9] Clarkson P A 2006 *Eur. J. Appl. Math.* **17** 293–322
- [10] Clarkson P A 2008 *Anal. Appl.* **6** 349–69
- [11] Clarkson P A 2009 *Nonlinear Anal.: Real World Appl.* **10** 3360–71
- [12] Dudley J M, Genty G, Dias F, Kibler B and Akhmediev N 2009 *Opt. Express* **17** 21497–508
- [13] Ganshin A N, Efimov V B, Kolmakov G V, Mezhov-Deglin L P and McClintock P V E 2008 *Phys. Rev. Lett.* **101** 065303
- [14] Hone A N W 1997 *J. Phys. A: Math. Gen.* **30** 7473–83
- [15] Montina A, Bortolozzo U, Residori S and Arecchi F T 2009 *Phys. Rev. Lett.* **103** 173901
- [16] Müller P, Garrett C and Osborne A 2005 *Oceanography* **18** 66–75
- [17] Nakamura A and Hirota R 1985 *J. Phys. Soc. Japan* **54** 491–9
- [18] Noumi M and Yamada Y 1999 *Nagoya Math. J.* **153** 53–86
- [19] Peregrine D H 1983 *J. Aust. Math. Soc. B* **25** 16–43
- [20] Solli D R, Ropers C, Koonath P and Jalali B 2007 *Nature* **450** 1054
- [21] Stenflo L and Marklund M 2010 *J. Plasma Phys.* arXiv:0911.1654 submitted
- [22] Yan Z 2009 Financial rogue waves arXiv:0911.4251
- [23] Zakharov V E 1968 *J. Appl. Mech. Tech. Phys.* **9** 190–4